DOI: 10.1002/ejic.200500975

Facile Synthesis of SnO_2 Hollow Nanospheres and Applications in Gas Sensors and Electrocatalysts

Qingrui Zhao,[a] Yang Gao,[a] Xue Bai,[a] Changzheng Wu,[a] and Yi Xie*[a]

Keywords: Tin oxides / Room-temperature sensitivity / Electrocatalysts

Tin oxide (SnO_2) hollow nanospheres have been successfully synthesized from mixed ethanol and water systems containing the surfactants sodium dodecyl benzenesulfonate (SDBS) and terephthalic acid. Systematic studies reveal that terephthalic acid plays pivotal roles in the formation of hollow nanospheres. In the present work, the as-synthesized SnO_2 hollow nanospheres exhibit excellent room-temperature ethanol sensitivity and potential catalytic ability towards the electrooxidation of ethanol, and thus are expected to be economical alternative catalysts and useful in industrial applications such as room-temperature gas sensors.

Introduction

Tin oxide (SnO_2), an n-type semiconductor with a wide bandgap (E_g = 3.62 eV), is a key functional material, which has attracted a lot of interest as an excellent candidate for optoelectronic devices,[1] gas sensors,[2] transparent conducting electrodes,[3] and catalyst supports.[4] With specific morphologies, the hollow structures are more desirable because of their potential for encapsulation of large quantities of guest molecules or large-sized guests within the empty core domain.[5] For example, hollow SnO_2 microspheres offer enhancement in sensitivity to methanol, carbon monoxide, benzene, and water over compact chemical vapor deposition (CVD) films at high temperatures.[6] On the basis of this, hollow spheres of SnO_2 have been produced with sizes ranging in the submicrometer regime. For example, Xia et al. used polystyrene particles as templates to fabricate mesoscale hollow spheres of SnO_2 with an average diameter of 400 nm.[7] Qian et al. synthesized SnO_2 hollow microspheres with a diameter of several micrometers by hydrolysis of $SnCl_4$ in alkaline media.[8]

Although various types of gas sensors have been investigated, great effort has focused on exploring the high temperature sensitivity of sensors.[9] However, the sensors working at lower temperatures, especially room temperature, no doubt have wider and more practical applications such as in the detection of drunk drivers by measuring ethanol concentrations of their breath. Therefore, it becomes more important to explore the room-temperature sensitivity of SnO_2. One useful strategy for increasing the poor sensitivity of tin oxide at room temperature may be realized by controlling the morphology as well as decreasing the size of the sensor materials. However, little work has been reported on the production of hollow SnO_2 nanospheres, which are expected to show superior properties. Thus, the exploration of a simple and easily scaled-up route to hollow nanostructures is still a great challenge so far.

Tin oxide materials have been known for a long time to display good catalytic activity towards the synthesis of vinyl ketone,[10] oxidation of methanol,[11] and so on. Recently, the demands for alternative energy sources such as fuel cells have attracted great interest in the studies on nanostructured materials. Among various candidates for catalysts of ethanol fuel cells, carbon-supported $PtSnO_2$ catalysts have exhibited excellent catalytic activity for ethanol electrooxidation, in which SnO_2 can enhance the catalytic activity for alcohol electrooxidation.[11] Therefore, nanomaterials with SnO_2 alone are believed to display potential catalytic activity for ethanol electrooxidation. In this paper, the electrochemical properties of the prepared hollow SnO_2 nanospheres for ethanol electrooxidation were examined.

Among many preparative methods for hollow nano- and mesoscaled structures, template-assisted synthesis is an effective approach in which hard templates[12,13] and soft templates[14] have been utilized. Surfactants tend to self-assemble to form micelles with desired structures and have been widely used as soft templates.[15] However, in many systems, the aggregated micelles may be very sensitive to the solvents and become unstable, which may not facilitate their use as templates in the microreactors. Thus, the complex surfactant systems are introduced to fabricate hollow structures.[16,17] For example, Qi et al. reported the synthesis of micrometer-sized hollow $CaCO_3$ spheres by using the complex surfactant of poly(ethylene oxide)-*block*-poly(methacrylic acid)–sodium dodecylsulfate (PEO-*b*-PMAA-

[a] Nano-materials and Nano-chemistry, Hefei National Laboratory for Physical Sciences at Microscale, University of Science & Technology of China,
Hefei, Anhui 230026, P. R. China
Fax: +86-551-3603987
E-mail: yxielab@ustc.edu.cn

SDS) micelles as templates,[16] in which the additive of PEO-*b*-PMAA could hold Ca^{2+} ions and assisted with the precipitation of $CaCO_3$. However, the large steric hindrance of the surfactant polymer PEO-*b*-PMAA-SDS made it difficult to restrict the size to the nanometer regime. Here, we suppose a simple coordination agent, which can hold metal ions without the large steric hindrance, may help to increase the stability of the soft template and thus further increase the formation of the hollow nanospheres. SnO_2 hollow nanospheres are successfully synthesized from a micelle system that is made up of the surfactants terephthalic acid along with sodium dodecyl benzenesulfonate (SDBS) in an ethanol and water (volume ratio 1:1) solution. Terephthalic acid can hold Sn^{2+} ions without a large steric hindrance, which is helpful for the growth of SnO_2 hollow nanospheres. We found that the as-synthesized SnO_2 hollow nanospheres show good room-temperature sensitivity to ethanol vapors and potential catalytic activity for electrooxidation of ethanol, which offers promising applications in the fields involving sensors and catalysts.

Results and Discussion

The phase and purity of the sample was determined by X-ray powder diffraction (XRD), and the typical diffraction pattern is shown in Figure 1. All the peaks were readily indexed to the tetragonal phase of SnO_2 (JCPDS card No. 41-1445), with lattice constants of a = 4.738 Å and c = 3.187 Å. No characteristic peaks were observed for the other impurities.

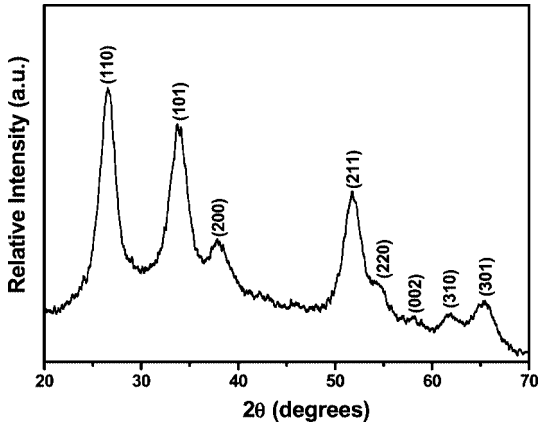

Figure 1. XRD pattern of the SnO_2 hollow nanospheres.

To further characterize the product, XPS was carried out to investigate the surface compositions and chemical state of the as-prepared products, and the results are shown in Figure 2. The binding energies obtained in the XPS analysis were corrected for specimen charging by referencing C_{1s} to 284.75 eV. The sample appeared as a spin-orbit doublet at ca. 486.85 eV ($3d_{5/2}$) and ca. 495.25 eV ($3d_{3/2}$) (Figure 2, a), which is in agreement with the reported value in the literature.[18] The O_{1s} binding energy of 531.00 eV (Figure 2, b) indicates that the oxygen atoms exist as O^{2-} species in the compounds. Quantification gave the atomic ratio of O and Sn elements as 1.93 on the basis of the areas of the O and Sn peaks within experimental error. Consequently, from the results of the XRD and XPS measurements the as-synthesized products could be determined as SnO_2.

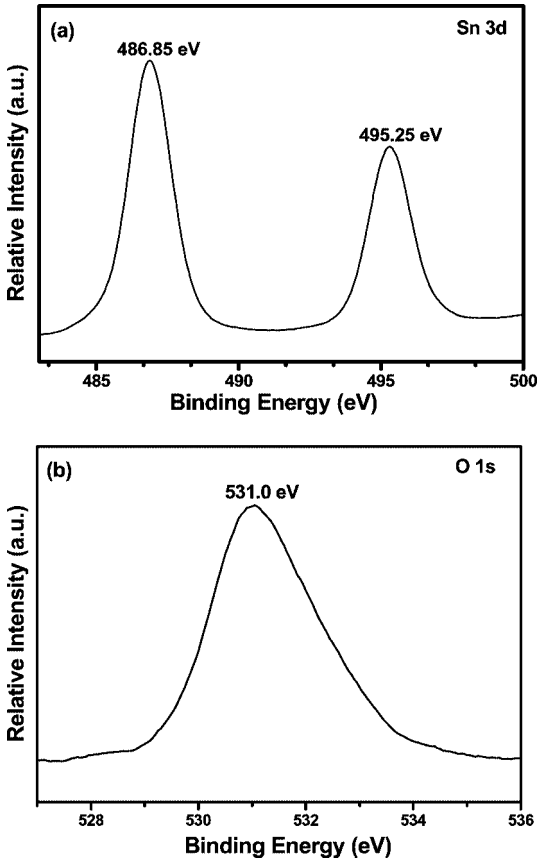

Figure 2. XPS spectra of the SnO_2 hollow nanospheres: (a) Sn region; (b) O region.

The structure and morphology of these hollow SnO_2 nanostructures were investigated by TEM. From the panoramic morphology shown in Figure 3 (a), a bright contrast (dark/bright) between the boundary and the center of the spheres is seen, confirming their hollow nature. The external diameter of the hollow spheres is 80–120 nm and the thickness of the shell is ca. 10–20 nm. The inset in Figure 3 (a) corresponds to the SAED pattern performed on the shell, and the circular character indicates the polycrystalline SnO_2 shell. The structural details were investigated from a high-magnification TEM image (Figure 3, b), revealing that the shells of hollow SnO_2 nanospheres seem to be rough and consist of nanoparticles with sizes in the range of 3–5 nm. The high-resolution transmission electron microscopy (HRTEM) images (Figure 3, c) further confirm the hollow nanostructures. FE-SEM observations also revealed that the SnO_2 nanospheres are hollow, which was learned from the broken regions of the spheres, as indicated by the arrows (see part d of Figure 3 and the inset).

It is known that SDBS is an anionic surfactant, which tends to self-assemble to form aggregates and further lead to the formation of microemulsions with desired structures because of its bulky hydrophobic tail compared with the

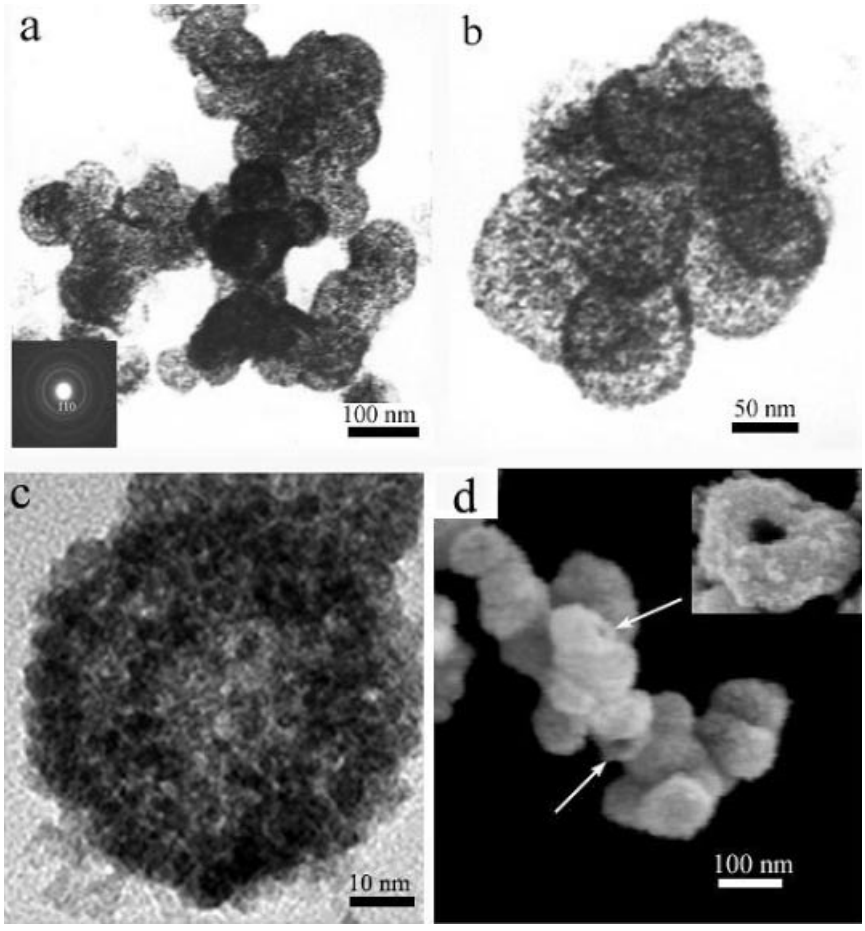

Figure 3. Electron microscopy images of the SnO_2 nanostructures. (a) TEM images. The inset in (a) is the corresponding ED pattern; (b) High-magnification TEM image; (c) HRTEM image of an individual SnO_2 hollow nanosphere; (d) FESEM image. The upper inset is the FESEM image of the 'opened' structure of a hollow sphere.

hydrophilic group.[19] However, in many systems SDBS micelles become unstable. Thus, terephthalic acid is added to play the important role of facilitating the formation of more stable aggregates to provide chemical microenviroments. Previous investigations of the interaction between SDS, poly(ethylene glycol) (PEG), and poly(methacrylic acid) (PMAA) showed that ionic headgroups of SDS repelled the charged PMAA chains and only hydrocarbon chains of SDS partitioned into the PEG core of the polymer aggregates. Then PMAA as a shell may be adsorbed onto the surface of the core, which is made up of PEG and SDS, through the interaction between the PMAA and PEG.[20] Thus, we could speculate that the mixture of SDBS and terephthalic acid in the mixed ethanol and water solutions could form complex micelles similar to that of the PEG-PMAA-SDS complex. In this case, ethanol with ethyl and ethylene oxide groups could interact with anionic SDBS to form micelles.[21] Terephthalic acid as a shell might be adsorbed onto the surface of the micelles through the interaction between ethanol and terephthalic acid. Such micelles would function as soft templates and provide the microenviroment in which nucleation and growth of SnO_2 could occur. In this approach, SnO_2 was synthesized by the chemical reaction of $SnCl_2$ and $KClO_3$ in ethanol and water solutions of terephthalic acid and SDBS, on the basis of the following equation:

$$3\,Sn^{2+} + ClO_3^- + 3\,H_2O \rightarrow 3\,SnO_2 + Cl^- + 6\,H^+$$

Terephthalic acid provides the nucleation sites for the crystallization of SnO_2 owing to the interaction of terephthalic acid and Sn^{2+}, which leads to a high local supersaturation of Sn^{2+} over the micelle periphery.[20] The crystallization of SnO_2 started from these nucleation sites on the surface of the micelles and the crystals developed outwards until they collided with each other, leading to the final hollow structures. A schematic pattern of the formation process was shown in Scheme 1. It is worth noting that the SnO_2 hollow nanospheres, which are attributed to the simple coordination agent terephthalic acid that can hold Sn^{2+} ions, formed without a large steric hindrance.

The complex surfactant system was critical in the formation of hollow nanospheres. If the reaction was carried out in the absence of terephthalic acid the products were found to be large amounts of SnO_2 nanoparticles and a few hollow nanospheres; whereas if the experiment was carried out without SDBS under similar conditions, only SnO_2 nanoparticles were obtained. The results above indicate that single SDBS-micelles as soft templates ae unstable, but the presence of terephthalic acid favored the formation of stable

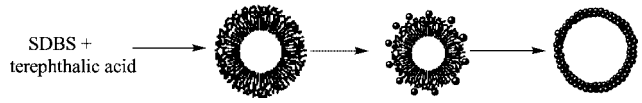

Scheme 1. Schematic illustration of the formation process of SnO_2 hollow nanospheres: a mixture of SDBS and terephthalic acid complexes in the system → complex micelles were formed → SnO_2 particles formed on the surface of the micelles → SnO_2 hollow nanospheres emerged as the final product.

micelles, and thus further helped the growth of the SnO_2 hollow nanospheres. The synergistic effect of terephthalic acid and SDBS as the soft templates in the formation of SnO_2 hollow nanospheres has been confirmed.

It is known that the solvent composition has a great effect on the formation of the micelle structures.[15] The solvent composition influences the difference in solubility of the hydrophilic head and hydrophobic tail of the surfactant, thus affecting the formation and aggregation of the micelles. To investigate the effect of the solvent composition, a series of comparative experiments were carried out. When keeping other experimental conditions unchanged, the absence of ethanol would only produce irregular SnO_2 particles. When trace ethanol was introduced into the system, a few hollow nanospheres appeared in the products. If the volume ratio of ethanol and water was increased to 1:1 all the samples had a hollow nanosphere morphology. These results demonstrate that ethanol seems to perform the function of bridging the SDBS and terephthalic acid, which is consistent with the proposed mechanism above. Moreover, the addition of ethanol could have increased the solubility of terephthalic acid in this approach, which facilitated the formation of micelles and was necessary for the formation of SnO_2 hollow nanospheres. However, at a high percentage of the ethanol solvent only a few SnO_2 hollow nanospheres formed. This may be caused by the lower solubility of $KClO_3$ at a high ethanol percentage, leading to incomplete reaction.

The room-temperature PL spectrum of hollow SnO_2 nanospheres, as shown in Figure 4, was obtained with an excitation wavelength of 340 nm. It can be seen that the spectrum of the sample is characterized by one strong emission band at 410 nm. Earlier reports indicated that SnO_2 thin films exhibit a broad dominant peak near 396 nm (3.1 eV),[22] and that SnO_2 nanoribbons synthesized by self-catalyst growth have a strong emission band centered at ca. 500 nm because of other luminescence centers, such as crystal defects.[23] The newly observed peaks at 410 nm might result from other luminescence centers, such as oxygen vacancies or tin interstitials in the obtained hollow SnO_2 nanospheres.

The hollow structure of the SnO_2 hollow nanospheres was expected to offer advantages in fabricating gas sensors at room temperature. The room-temperature sensitivity of the obtained SnO_2 hollow nanospheres in response to C_2H_5OH was investigated, which is shown in Figure 5 (a). The gas sensitivity, S_g, was defined as R_{air}/R_{gas}, where R_{air} and R_{gas} are the electrical resistances for the sensor in air and in gas.[24] It can be seen from Figure 5 (a) that the sensitivity of the SnO_2 hollow nanospheres gradually increases with an increase in ethanol gas concentration. To evaluate the sensitivity of the SnO_2 hollow nanospheres, solid SnO_2 nanoparticles with a diameter of 5 nm were fabricated according to ref.[25] The room-temperature sensitivity of 5 nm SnO_2 nanoparticles is displayed in Figure 5 (b) and compared with that of the hollow nanospheres. As shown in Figure 5, the sensitivity of the SnO_2 hollow nanospheres versus ethanol concentration was much greater than that for the SnO_2 nanoparticles under the same conditions. For the sensors, we believe that the higher sensitivity might be attributed to the hollow structures of the sample, which has more chance to adsorb and desorb the gas molecules.[24] In addition, in order to test the reversibility of the sample, the measurements were repeated more than 10 times and no major changes in the signals were observed.

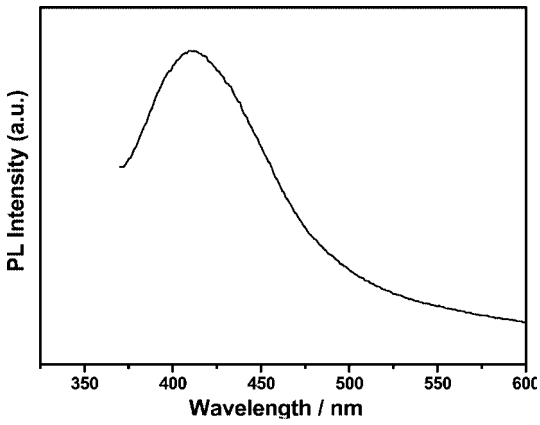

Figure 4. PL spectrum of the SnO_2 hollow nanospheres.

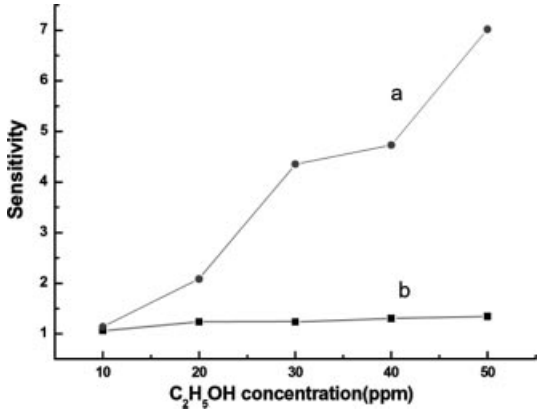

Figure 5. Room-temperature sensor sensitivity to ethanol of (a) the as-prepared SnO_2 hollow nanospheres and (b) nanoparticles.

Brunauer–Emmett–Teller (BET) nitrogen adsorption-desorption measurements showed that the surface area of the hollow SnO_2 nanospheres is 44 $m^2 g^{-1}$, whereas the surface area of SnO_2 nanoparticles is 31 $m^2 g^{-1}$. The small difference between the BET surface area of the SnO_2 hollow nanospheres and the nanoparticles may be attributed to the fact that the surface of the SnO_2 hollow nanospheres is composed of compact nanoparticles. The superior sensing properties of the obtained hollow SnO_2 nanospheres could

be because of its porous structure associated with the small grain size,[6] which enables ethanol gas to access almost all of the surfaces of the hollow SnO_2 nanospheres contained in the sensing unit. Therefore, hollow SnO_2 nanospheres with a higher surface area have more chances to adsorb and desorb ethanol gas molecules, which leads to higher sensitivity at room temperature.

In previous reports, SnO_2 nanoparticles were employed to synthesize the carbon-supported $PtSnO_2$ catalyst, which promoted catalytic activity of the ethanol electrooxidation in fuel cells.[11] However, a critical problem with Pt-based catalysts is their prohibitive cost. Therefore, economical and effective alternative catalysts are required. Thus, in the current work the electrooxidation of ethanol of SnO_2 hollow nanospheres was investigated without Pt, using a well-used electrochemical reaction in a solution of H_2SO_4,[26] and the result indicated that SnO_2 hollow nanospheres exhibit a good electrocatalytic performance for the electrooxidation of ethanol. Figure 6 shows the cyclic voltammetric responses of the bare glass carbon electrode (GCE) (a) and also the SnO_2 hollow nanospheres on the glass carbon electrode surface (b) in the presence of ethanol. From the voltammograms in Figure 6 (b), it can be seen that SnO_2 hollow nanospheres show catalytic behavior for electrooxidation of ethanol by the appearance of an oxidation current in the positive potential region. The peak potentials for the oxidation of ethanol were approximately 0.46 V, in agreement with the literature values of ethanol oxidation for the formation of acetaldehyde.[27,28] The electrochemical reaction can be described by the following equations:

$$SnO_2(CH_3CH_2OH)_{ads} \rightarrow SnO_2(CH_3CHO)_{ads} + 2\,H^+ + 2\,e^-$$

$$SnO_2(CH_3CHO)_{ads} \rightarrow CH_3CHO + SnO_2$$

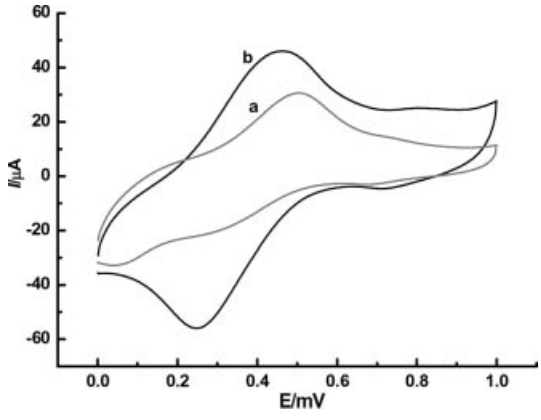

Figure 6. Cyclic voltammograms of the (a) bare glass carbon electrode and (b) SnO_2 hollow nanospheres on the glass carbon electrode surface in H_2SO_4 (0.5 M) and ethanol (0.6 M). Scan rate = 50 mV s^{-1}.

The scission of the alcohol bond occurred at the tin dioxide site with the breaking of the C–H bonds. The potential was about 40 mV more negative than the oxidation peak at the bare GCE. The peak currents of the hollow nanospheres loading onto the bare GCE and the bare GCE are 46 μA and 31 μA, respectively. The reduction of potential and the enhancement of the peak current indicates that the modified electrode can effectively catalyze the electrooxidation of ethanol. Most probably, the catalytic performance may be ascribed to the hollow structures. More chemicals (ions) can be stored in the hollow structures of the sample with a greater chance of participating in the reactions, thus greatly improving the catalytic efficiency of the obtained nanostructures. To test the recycling performance of the sample, two runs were reperformed under the same conditions. It was found that the catalytic efficiency in the third cycle was still the same, revealing its excellent recycling performance. Therefore, the SnO_2 hollow nanospheres exhibited potential catalytic behavior for the electrooxidation of ethanol.

Conclusions

The present study describes a micelle system for the preparation of SnO_2 hollow nanospheres on a large scale, which is made up of SDBS and terephthalic acid in mixed ethanol and water solutions. Their cooperative functions contribute to the final morphology of the SnO_2 hollow nanospheres. Such a system may represent a promising microreactor for the synthesis of other inorganic materials with unique properties. The obtained SnO_2 hollow nanospheres exhibit not only good room-temperature sensitivity to ethanol, but also potential electrocatalytic activity towards electrooxidation of ethanol, which may be useful in industrial applications including catalytic nanoreactors and gas sensors.

Experimental Section

In a typical experimental process, sodium dodecyl benzenesulfonate (SDBS) (1.4 g, 4 mmol) in distilled water (25 mL) and terephthalic acid (0.3 g, 2 mmol) in ethanol (25 mL) were loaded into a 60 mL Teflon-lined stainless steel autoclave, which was stirred for half an hour. Then $SnCl_2$ (0.45 g, 2 mmol) and $KClO_3$ (0.49 g, 4 mmol) were added under constant stirring to the solution to form a homogeneous solution, which was maintained at 180 °C for 12 h. After the reaction was completed, the white products were collected from solution, rinsed several times with distilled water and absolute ethanol, and then dried under vacuum at 40 °C for 4 h.

The samples were characterized by X-ray powder diffraction (XRD) with a Japan Rigaku D/max rA X-ray diffractometer equipped with graphite-monochromatized high-intensity Cu-K_α radiation (λ = 1.54178 Å), recorded with 2θ ranging from 10 to 70°. The transmission electron microscopy (TEM) images and electron diffraction (ED) patterns were performed with a Hitachi Model H-800 instrument with a tungsten filament, using an accelerating voltage of 200 kV. High-resolution transmission electron microscopy (HRTEM) images were carried out with a JEOL-2010 TEM at an acceleration voltage of 200 kV. The field emission scanning electron microscopy (FE-SEM) images were taken with a FEI Sirion-200 SEM. XPS was performed with a ESCALAB MKII with Mg-K_α ($h\nu$ = 1253.6 eV) as the excitation source. The binding energies obtained from the XPS spectral analysis were corrected for specimen charging by referencing C_{1s} to 284.75 eV. The room-temperature photoluminescence (PL) spectra were performed with a Jobin Yvon-Labram Steady-State/Lifetime Spectrofluorometer with a He-Cd laser. Gas-sensing measurements were performed with a

WS-30A system (Weisheng Instruments Co., Zhengzhou, China). Brunauer–Emmett–Teller (BET) surface area measurements was performed with a Micromeritics ASAP-2000 nitrogen adsorption apparatus. The as-prepared samples were cast as a thin film spanning across the two gold electrodes for test. Electrochemical measurements were performed with a CHI 832 electrochemical station (ChenHua Instruments Co., Shanghai, China). A conventional three-electrode system was used, consisting of a glassy carbon (4 mm diameter) working electrode (GCE), platinum wire auxiliary electrode, and a saturated calomel reference electrode (SCE). The working electrode was polished with Al_2O_3 paste and washed ultrasonically in distilled water, loading 0.3 mg cm^{-2}. Electrocatalytic oxidation measurements were carried out in a solution of H_2SO_4 (0.5 M) and ethanol (0.6 M).

Acknowledgments

This work was supported by the National Natural Science Foundation of China and Chinese Ministry of Education.

[1] J. S. Lee, S. K. Sim, B. Min, K. Cho, S. W. Kim, S. Kim, *J. Crystal. Growth* **2004**, *267*, 145–149.
[2] a) G. Faglia, C. Baratto, G. Sberveglieri, *Appl. Phys. Lett.* **2005**, *86*, 11923; b) G. Xu, Y. W. Zhang, X. Sun, C. L. Xu, C. H. Yan, *J. Phys. Chem. B* **2005**, *109*, 3269–3278.
[3] a) Y. Wang, J. Y. Lee, *J. Phys. Chem. B* **2004**, *108*, 17832–17837; b) H. Sugimoto, H. Tsukube, K. Tanaka, *Eur. J. Inorg. Chem.* **2004**, 4550–4553.
[4] N. Q. Jia, Q. Zhou, L. Liu, M. M. Yan, Z. Y. Jiang, *J. Electroanal. Chem.* **2005**, *580*, 213–221.
[5] Y. Xie, J. X. Huang, B. Li, Y. Liu, Y. T. Qian, *Adv. Mater.* **2000**, *12*, 1523–1526.
[6] C. J. Martinez, B. Hockey, C. B. Montgomery, S. Semancik, *Langmuir* **2005**, *21*, 7937–7944.
[7] Z. Y. Zhong, Y. D. Yin, B. Gates, Y. N. Xia, *Adv. Mater.* **2000**, *12*, 206–209.
[8] W. P. Shao, Z. H. Wang, Y. G. Zhang, J. H. Cui, W. C. Yu, Y. T. Qian, *Chem. Lett.* **2005**, *34*, 556–557.
[9] Z. A. Ansari, T. G. Ko, J. H. Oh, *IEEE Sensors J.* **2005**, *5*, 817–824.
[10] N. L. V. Carreno, H. V. Fajardo, A. P. Maciel, A. Valentini, F. M. Pontes, L. F. D. Probst, E. R. Lrite, E. Longo, *J. Molecular Catalysis A: Chem.* **2004**, *207*, 89–94.
[11] L. H. Jiang, G. Q. Sun, Z. H. Zhou, S. G. Sun, Q. Wang, S. Y. Yan, H. Q. Li, J. Tian, J. S. Guo, B. Zhou, Q. Xin, *J. Phys. Chem. B* **2005**, *109*, 8774–8778.
[12] a) M. L. Breen, A. D. Dinsmore, R. H. Pink, S. B. Qadri, B. R. Ratna, *Langmuir* **2001**, *17*, 903–907; b) Z. Yang, Z. Niu, Y. Lu, Z. Hu, C. C. Han, *Angew. Chem. Int. Ed.* **2003**, *42*, 1943–1945.
[13] a) Z. Dai, L. Dahne, H. Mohwald, B. Tiersch, *Angew. Chem. Int. Ed.* **2002**, *41*, 4019–4022; b) K. P. Velikov, A. van Blaaderen, *Langmuir* **2001**, *17*, 4779–4786.
[14] a) Y. J. Xiong, Y. Xie, J. Yang, R. Zhang, C. Z. Wu, G. A. Du, *J. Mater. Chem.* **2002**, *12*, 3712–3716; b) H. G. Yang, H. C. Zeng, *Angew. Chem. Int. Ed.* **2004**, *43*, 5206–5209.
[15] D. Chen, G. Z. Shen, K. B. Tang, Z. H. Liang, H. G. Zheng, *J. Phys. Chem. B* **2004**, *108*, 11280–11284.
[16] L. M. Qi, J. Li, J. M. Ma, *Adv. Mater.* **2002**, *14*, 300–303.
[17] D. B. Zhang, L. M. Qi, J. M. Ma, H. M. Cheng, *Adv. Mater.* **2002**, *14*, 1499–1502.
[18] H. J. Ahn, H. C. Choi, K. W. Park, S. B. Kim, Y. E. Sun, *J. Phys. Chem. B* **2004**, *108*, 9815–9820.
[19] T. Namani, P. Walde, *Langmuir* **2005**, *21*, 6210–6219.
[20] S. G. Deng, J. M. Cao, J. Feng, J. Guo, B. Q. Fang, M. B. Zheng, J. Tao, *J. Phys. Chem. B* **2005**, *109*, 11473–11477.
[21] G. Wang, G. Olofsson, *J. Phys. Chem. B* **1998**, *102*, 9276–9283.
[22] T. W. Kim, D. U. Lee, Y. S. Yoon, *J. Appl. Phys.* **2000**, *88*, 3759–3761.
[23] a) J. Q. Hu, Y. Bando, Q. L. Liu, D. Golberg, *Chem. Phys. Lett.* **2003**, *372*, 758–762; b) J. Q. Hu, Y. Bando, Q. L. Liu, D. Golberg, *Adv. Funct. Mater.* **2003**, *13*, 493–496.
[24] J. Chen, L. N. Xu, W. Y. Li, X. H. Gou, *Adv. Mater.* **2005**, *17*, 582–586.
[25] J. J. Zhu, Z. H. Lu, S. T. Aruna, D. Aurbach, A. Gedanken, *Chem. Mater.* **2000**, *12*, 2557–2566.
[26] H. P. Liang, H. M. Zhang, J. S. Hu, Y. G. Guo, L. J. Wan, C. L. Bai, *Angew. Chem. Int. Ed.* **2004**, *43*, 1540–1543.
[27] L. H. Jiang, G. Q. Sun, Z. H. Zhou, W. J. Zhou, Q. Xin, *Catalysis Today* **2004**, *93–95*, 665–670.
[28] J. M. Leger, *Electrochim. Acta* **2005**, *50*, 3123–3129.

Received: November 3, 2005
Published Online: February 21, 2006

